doi:10.3788/gzxb20154401.0116001

应变纤锌矿 ZnO/$Mg_xZn_{1-x}O$ 盘形量子点中的离子施主束缚激子态

郑冬梅,王宗篪
(三明学院 机电工程学院,福建 三明 365004)

摘 要:在有效质量近似下,计算了盘形量子点中离子施主束缚激子的结合能、光跃迁能、振子强度及辐射寿命.设盘形量子点由有限长的柱形 ZnO 材料组成,四周被 $Mg_xZn_{1-x}O$ 包围,离子施主局域在盘轴.考虑了由于自发极化和压电极化引起的内建电场效应,并在有限深约束势下采用合适的变分波函数进行.计算结果表明,量子盘结构参数(盘高度及垒中 Mg 组分)和离子施主的位置对离子施主束缚激子的结合能、光跃迁能、振子强度及辐射寿命有强烈的影响.随着盘高度的增加,结合能、光跃迁能和振子强度减小,而辐射寿命增加.对含 Mg 量较高的盘形量子点,盘高度对结合能、光跃迁能、振子强度及辐射寿命的影响更显著.当施主杂质位于量子点的左界面附近时结合能(光跃迁能)有极大(极小)值,而当施主杂质位于量子点的右界面附近时结合能(光跃迁能)有极小(极大)值.

关键词:ZnO 量子点;离子施主束缚激子;结合能;光跃迁能;振子强度;辐射寿命
中图分类号:$O472^+.3$ **文献标识码**:A **文章编号**:1004-4213(2015)01-0116001-8

Ionized Donor Bound Exciton States in Strained Wurtzite ZnO/$Mg_xZn_{1-x}O$ Disk-shaped Quantum Dots

ZHENG Dong-mei, WANG Zong-chi
(*College of Electromechanical Engineering, Sanming University, Sanming, Fujian* 365004, *China*)

Abstract: Within the framework of the effective-mass approximation, the binding energy, optical transition energy, oscillator strength, and radiative lifetime of ionized donor bound exciton (D^+X) in a Quantum Dot (QD) were calculated, assumed that the ionized donor was located at the disk axis, the disk-shaped QD consisted of a finite length cylinder of ZnO material surrounded by $Mg_xZn_{1-x}O$. The calculations were performed by using a suitable variational wave function for finite confinement potential at all surfaces, including the strong built-in electric field effect due to the spontaneous and piezoelectric polarizations. Calculated results reveal that the disk structural parameters (height and Mg composition in the barrier) and the donor position have a strong influence on the binding energy, optical transition energy, oscillator strength, and radiative lifetime of (D^+X) complex. As the disk height increases, the binding energy, optical transition energy, and oscillator strength both decrease, whereas the radiative lifetime increases. The influences of disk height on the binding energy, optical transition energy, oscillator strength, and radiative lifetime become more prominent for the QDs with higher Mg composition. The binding energy (the optical transition energy) has a maximum (minimum) when the donor is located in the vicinity of the left interface of the QDs. On the contrary, the binding energy (the optical transition energy) has a minimum (maximum) when the donor is located in the vicinity of the right interface of the QDs.

Key words: ZnO quantum dot; Ionized donor bound exciton; Binding energy; Optical transition energy;

Foundation item: The National Natural Science Foundation for Young Scientists of China (No. 11102100)
First author: ZHENG Dong-mei (1971—), female, professor, mainly focuses on the theoretical study of the properties of the wide-band gap semiconductor material. Email:smdmzheng@sina.com
Received: Aug. 6, 2014; **Accepted**: Sep. 23, 2014

Oscillator strength; Radiative lifetime
OCIS Codes: 160.6000; 160.4760; 020.4900

0 Introduction

ZnO is widely investigated as a potential photoelectric material because of the large band gap of 3.37 eV and large exciton binging energy of 60 meV at room temperature. Moreover, doping Mg, Co, and Mn, etc. in ZnO and studying the properties of ZnO alloy is an interesting subject[1-4]. For example, extensive experimental work has been devoted to the subject of fabricating and studying ZnO/Mg_xZn_{1-x}O superlattices because of the novel properties compared to GaN/Al_xGa_{1-x}N superlattices[5-8]. Optical properties of Wurtzite (WZ) ZnO/MgZnO Quantum Wells (QWs) have been investigated extensively[9-13]. Also, it was reported that there exists a large built-in electric field (BEF) due to Spontaneous (SP) and Piezoelectric (PE) polarizations in WZ ZnO/MgZnO QW structures[14-15], Morhain, *et al*[13,16]. reported on the determination of a value of 0.9 MV/cm for BEF in ZnO/$Zn_{0.78}Mg_{0.22}$O QWs, and led the BEF by linear interpolation to a maximum field of 4.1x for ZnO/Mg_xZn_{1-x}O QWs. Therefore, optical properties of [0001]-oriented WZ ZnO/MgZnO strained QWs are strongly affected by the BEF due to the Quantum-Confined Stark Effect (QCSE). Furthermore, it was found that ZnO Quantum Dots (QDs) have much higher photoluminescence quantum efficiency than their bulk counterpart[17-18]. Therefore, WZ ZnO/MgZnO QD is expected to have more possible advantages in optoelectronic devices. Lately, the excitonic states and the interband transitions in WZ ZnO/MgZnO QDs have been investigated theoretically with the inclusion of internal electric field by means of a variational approach within the framework of the effective-mass approximation[19-23].

It is well known that impurity states play a very important role in some semiconductor optoelectronic devices. Without impurities, there would be no diode, no transistor, or any semiconductor science and technology. A deep understanding of the effects of impurities on exciton states of semiconductor nanostructures is a fundamental question in semiconductor physics, because their presence can dramatically alter the performance of quantum devices. Recently, the optical transitions due to donor bound exciton (D^0X) (D^+X) and acceptor bound exciton (A^0X) (A^-X) in ZnO epitaxial layers have been observed at low temperature[24-32]. Therefore, studying bound exciton states and related interband optical transitions in the metal oxide-based nanostructures is an issue of great importance in the understanding of optical properties and practical applications of these oxides. To the best of our knowledge, there is little theoretical and experimental work on the bound exciton states in the WZ ZnO/Mg_xZn_{1-x}O QD so far. Consequently, it is necessary and imperative to investigate the bound exciton states confined in WZ ZnO/Mg_xZn_{1-x}O QDs in detail. In this paper, we are going to focus on the simplest bound exciton system (D^+X) confined in strained WZ ZnO/Mg_xZn_{1-x}O disk-shaped QDs, consisting of an electron and a hole bound to an ionized positively charged donor. We investigate the luminescent properties of the (D^+X) complex as functions of the disk structural parameters (height, radius, and Mg composition in the barrier) and the donor position, within the framework of the effective-mass approximation and by means of a variational method. Moreover, the effect of the strong BEF due to the SP and PE polarizations is also included.

1 Model and theory

We consider an isolated WZ ZnO disk-shaped QD with radius R and height L, surrounded by large energy gap materials WZ $Mg_xZn_{1-x}O$ in both radius and z-direction, in which the origin is taken at the center of the disk-shaped QD and the z axis is defined to be the growth direction (Fig. 1). For simplicity, we assume that the width of the barrier is much larger than the disk height (i.e., $L^{Mg_xZn_{1-x}O} \gg L^{ZnO}$). Here, adopt a cylindrical coordinate system, the coordinates of electron, hole and donor are denoted by (ρ_e, φ_e, z_e),

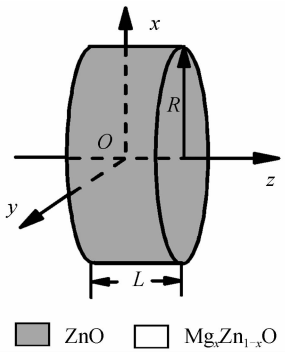

Fig. 1 A diagram of a WZ ZnO disk-shaped QD embedded in an infinite WZ $Mg_xZn_{1-x}O$ matrix

(ρ_h, φ_h, z_h), and (0, 0, z_0), respectively. Within the effective-mass approximation, the Hamiltonian of (D^+X) complex in a strained WZ ZnO/Mg_xZn_{1-x}O disk-shaped QD can be written as

$$\hat{H}_{(D^+X)} = \sum_{j=e,h}\left\{-\frac{\hbar^2}{2m_j^*}\left[\frac{1}{\rho_j}\frac{\partial}{\partial\rho_j}\left(\rho_j\frac{\partial}{\partial\rho_j}\right)+\frac{1}{\rho_j^2}\frac{\partial^2}{\partial\theta_j^2}+\frac{\partial^2}{\partial z_j^2}\right]+V(\rho_j,z_j)\mp eFz_j\right\}+E_{g,ZnO}-$$

$$\frac{e^2}{4\pi\varepsilon_0\bar{\varepsilon}}\left(\frac{1}{|\boldsymbol{r}_e-\boldsymbol{r}_h|}+\frac{1}{|\boldsymbol{r}_e-\boldsymbol{r}_0|}-\frac{1}{|\boldsymbol{r}_h-\boldsymbol{r}_0|}\right) \quad (1)$$

where $E_{g,\mathrm{ZnO}}$ is the band gap energy of the WZ ZnO material, $\boldsymbol{r}_e$, $\boldsymbol{r}_h$, and $\boldsymbol{r}_0$ are the position vectors of the electron, hole, and donor, respectively. m_j^* is the electron (hole) effective mass, ε_0 is the permittivity of free space, and $\bar{\varepsilon}$ is the effective mean relative dielectric constant of the embedding material between the electron and hole. $V(\rho_j, z_j)$ is the electron (hole) confinement potential due to the band offset (Q_j) and is given by

$$V(\rho_j,z_j)=\begin{cases}V(\rho_j), |z_j|\leqslant\dfrac{L}{2}\\ Q_j[E_{g,\mathrm{Mg}_x\mathrm{Zn}_{1-x}\mathrm{O}}-E_{g,\mathrm{ZnO}}], |z_j|>\dfrac{L}{2}\end{cases} \quad (2)$$

$$V(\rho_j)=\begin{cases}0,\rho_j\leqslant R\\ Q_j[E_{g,\mathrm{Mg}_x\mathrm{Zn}_{1-x}\mathrm{O}}-E_{g,\mathrm{ZnO}}],\rho_j>R\end{cases} \quad (3)$$

In this paper, the ratio of the conduction band to the valence band offset is assumed to be 65:35[15].

The strength of the BEF due to the SP and PE polarizations along the growth direction is given by[22]

$$\begin{cases}F^{\mathrm{ZnO}}=\left|-\dfrac{P_{\mathrm{SP}}^{\mathrm{ZnO}}+P_{\mathrm{PE}}^{\mathrm{ZnO}}-P_{\mathrm{SP}}^{\mathrm{Mg}_x\mathrm{Zn}_{1-x}\mathrm{O}}}{\varepsilon_e^{\mathrm{ZnO}}\varepsilon_0}\right|\\ F^{\mathrm{Mg}_x\mathrm{Zn}_{1-x}O}\to 0\end{cases} \quad (4)$$

where F^{ν} (ν=ZnO or $Mg_xZn_{1-x}O$) denotes the BEF of layer ν, P_{SP}^{ν} is the SP polarization in the equilibrium lattice, P_{PE}^{ν} is the PE polarization, and ε_e^{ν} is the electronic dielectric constant of material ν, which is different from the static dielectric constant of layer ν. Generally speaking, the direction of the BEF depends on the orientation of the piezoelectricity and SP polarization, and also the BEF is determined by both the polarity of crystal and the strain of disk-shaped QD structures.

The wave function of the uncorrelated electron (hole) confined in our WZ ZnO/$Mg_xZn_{1-x}O$ disk-shaped QD potentials Eqs. (2) and (3) can be written as

$$\psi_j(\rho_j,\varphi_j,z_j)=f(\rho_j)h(z_j)e^{im\varphi_j},m=0,\pm1,\pm2,\cdots \quad (5)$$

where m is the electron (hole) z-component angular momentum quantum number. The radial wave function $f(\rho_j)$ and the corresponding confinement energy equation of the electron (hole) can be obtained using the m-order Bessel function J_m and the modified Bessel function K_m. For the z-axis motion of the electron (hole), the wave function $h(z_j)$ and the related confinement energy equation can be expressed by means of the Airy functions Ai and Bi.

Here, we adopt the variational approach to estimate the ground-state binding energy of (D^+X) and wave function. As in the previous works, we choose a trial wave function of the following form[33-34]

$$\Phi_{(D^+X)}(\boldsymbol{r}_e,\boldsymbol{r}_h)=\psi_e(\rho_e,\varphi_e,z_e)\psi_h(\rho_h,\varphi_h,z_h)e^{-\alpha\rho_{eh}^2}e^{-\beta z_{eh}^2} \quad (6)$$

where $\rho_{eh}^2=\rho_e^2+\rho_h^2-2\rho_e\rho_h\cos(\varphi_e-\varphi_h)$, $z_{eh}^2=(z_e-z_h)^2$. In Eq. (6), the variational parameter α is responsible for the in-plane correlation, and β accounts for the correlation of the relative motion in the z-direction.

The ground-state energy of (D^+X) $E_{(D+X)}$ in the WZ ZnO/Mg_xZn_{1-x}O disk-shaped QDs can be determined by

$$E_{(D^+X)}=\min_{\alpha,\beta}\frac{\langle\Phi_{(D^+X)}|\hat{H}_{(D^+X)}|\Phi_{(D^+X)}\rangle}{\langle\Phi_{(D^+X)}|\Phi_{(D^+X)}\rangle} \quad (7)$$

The binding energy of (D^+X) E_b and the optical transition energy E_{ph} can be defined as follows,

$$E_b=E_e+E_h+E_{g,\mathrm{ZnO}}-E_{(D^+X)} \quad (8)$$

$$E_{ph}=E_e+E_h+E_{g,\mathrm{ZnO}}-E_b \quad (9)$$

where E_e (E_h) is the electron (hole) confinement energy in the WZ ZnO/$Mg_xZn_{1-x}O$ disk-shaped QDs.

The oscillator strength of (D^+X) state $f_{(D+X)}$ with energy $E_{(D+X)}$ and envelope wave function $\Phi_{(D+X)}(\boldsymbol{r}_e,\boldsymbol{r}_h)$ is calculated as[35-36]

$$f_{(D^+X)}=\frac{E_p}{E_{(D^+X)}}\left|\int d\boldsymbol{r}_e d\boldsymbol{r}_h\Phi_{(D^+X)}(\boldsymbol{r}_e,\boldsymbol{r}_h)\delta(\boldsymbol{r}_e-\boldsymbol{r}_h)\right|^2 \quad (10)$$

where the Kane energy of ZnO is E_p=28.2 eV[35]. The oscillator strength not only defines the strength of absorption lines, but also relates to the radiative lifetime τ[35-36]

$$\tau=\frac{2\pi\varepsilon_0 m_0 c^3\hbar^2}{ne^2E_{ph}^2f_{(D^+X)}} \quad (11)$$

where ε_0, m_0, c, $\hbar$, and e are fundamental physical constants with their usual meaning and n is the refractive index.

2 Results and discussion

In order to clarify the influences of the disk structural parameters (height L, radius R, and Mg composition x in the barrier) and the donor position on the (D^+X) states confined in strained WZ ZnO/$Mg_xZn_{1-x}O$ disk-shaped QDs, we have calculated the binding energy of (D^+X), optical transition energy, and oscillator strength, considering the strong BEF induced by the SP and the PE polarization. Moreover, we have further calculated the radiative lifetime of (D^+X). In the following numerical calculations, we ignore the effect of the complicated valence band structure of ZnO and $Mg_xZn_{1-x}O$. All material parameters used in the present article are the same as in Ref. [22].

Fig. 2 shows the binding energy of (D^+X) E_b and the optical transition energy E_{ph} calculated as a function of the disk height L in strained WZ ZnO/$Mg_xZn_{1-x}O$ disk-shaped QDs with radius R=10 nm for different Mg compositions when the ionized donor is located at the center of the disk-shaped QDs. From Fig. 2(a), we note that as the disk height L decreases the binding energy of (D^+X) grows up to a maximum and then

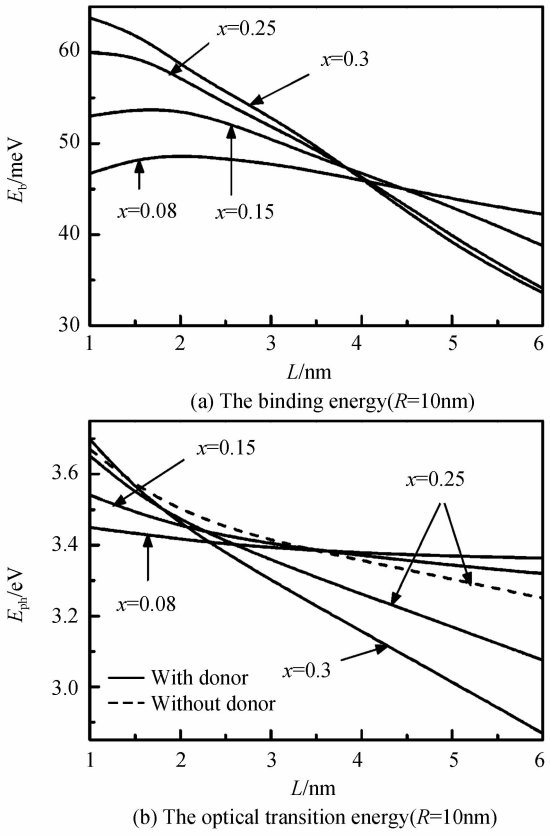

Fig. 2 Variations of the binding energy and optical transition energy as a function of disk height L when the donor is located at the center of the disk-shaped QDs

slowly drops if Mg composition is low ($x=0.08$ and 0.15), however, it increases monotonically with decreasing the disk height if Mg composition is high ($x=0.25$ and 0.3). Further, it is noticed that the variation tendency of the binding energy with the disk height is more prominent for the disk-shaped QDs with higher Mg composition. For the same disk height, E_b increases with the increasing Mg composition if the disk height $L<3.8$ nm, whereas E_b decreases with increasing Mg composition if the disk height $L>4.4$ nm. As we know, the binding energy of (D^+X) is an indication of the electron-hole Coulomb interaction when the donor is located at the center of the disk-shaped QDs. The well-known behavior of the increase in the binding energy of (D^+X) is associated with the reduction of mean relative distance in the z-direction between the electron and hole with decreasing the disk height. However, when Mg composition in the barrier is low ($x=0.08$ and 0.15), the contribution of potential barrier confinement is weak for smaller disk height, the electron (hole) wave function tunnels through the barrier, the Coulomb interaction between the electron and hole is reduced which ultimately causes the decrease in binding energy. Furthermore, as Mg composition increases: 1) the increase in the potential barrier height induces that the electron and hole wave functions are more strongly localized inside the QDs, this leads to an increase in the binding energy of (D^+X); 2) the intensity of the BEF in the strained ZnO layer is strengthened, the strong BEF induces the remarkable spatial separation of electron and hole, and leads to a reduction of the binding energy. When the disk height is small ($L<3.8$ nm), the first effect prevails, so the binding energy increases with the increase in Mg composition. On the contrary, the latter prevails if the disk height is large ($L>4.4$ nm), thus the binding energy decreases with increasing Mg composition. The results indicate that any quantum device depends on the composition of the barrier material and the spatial confinement of geometrical size.

From Fig. 2(b), we can see that the optical transition energy E_{ph} decreases monotonically as the disk height L increases. The reason is that the electron and hole confinement energies in ZnO/MgZnO strained disk-shaped QDs are decreased with the increase in the disk height. Further, the decreasing trend of E_{ph} with the increase of disk height is more obvious for the disk-shaped QDs with higher Mg composition, when Mg composition x increases to 0.3, the scope of optical transition energy is broadened and E_{ph} comes to 2.869 eV with $L=6$ nm which is far below the bulk WZ ZnO energy gap 3.37 eV. Mg composition in the barrier affects the optical transition energy by increasing the confinement potential of the electron and hole and increasing the electric field. Moreover, it is noticed from Fig. 2(b) that the incorporation of the ionized donor in the disk-shaped QDs can obviously reduce the optical transition energy, especially for the larger disk height. For example, at $L=2$ nm, the optical transition energy of ionized donor bound exciton is $E_{ph}=3.471\,5$ eV, whereas we obtain 3.499 9 eV for free exciton state withont the ionized donor. The deference is $\Delta E_{ph}=28.4$ meV. The difference $\Delta E_{ph}=174.3$ meV increases 6.14 times when L increases from 2 to 6 nm.

In Fig. 3, we present the variations of the binding energy of (D^+X) E_b and the optical transition energy E_{ph} as a function of disk radius in strained WZ ZnO/$Mg_xZn_{1-x}O$ disk-shaped QDs with height $L=2$ nm for different Mg compositions when the donor is located at the center of the disk-shaped QDs. It is seen from Fig. 3(a) that as the disk radius increases, the binding energy of (D^+X) decreases monotonically in all case. This is due to the increase of the in-plane mean relative distance between the electron and hole and weakening of the Coulomb interaction when R increases. Furthermore, Fig. 3(a) also show that the binding

energy of (D^+ X) increases with increasing Mg composition for any disk radius when the disk height $L=2$ nm. The main reason is that the increase in the potential barrier height due to the increasing Mg composition induces that the electron and hole wave functions are more strongly localized inside the disk-shaped QDs which ultimately causes the increase in the binding energy.

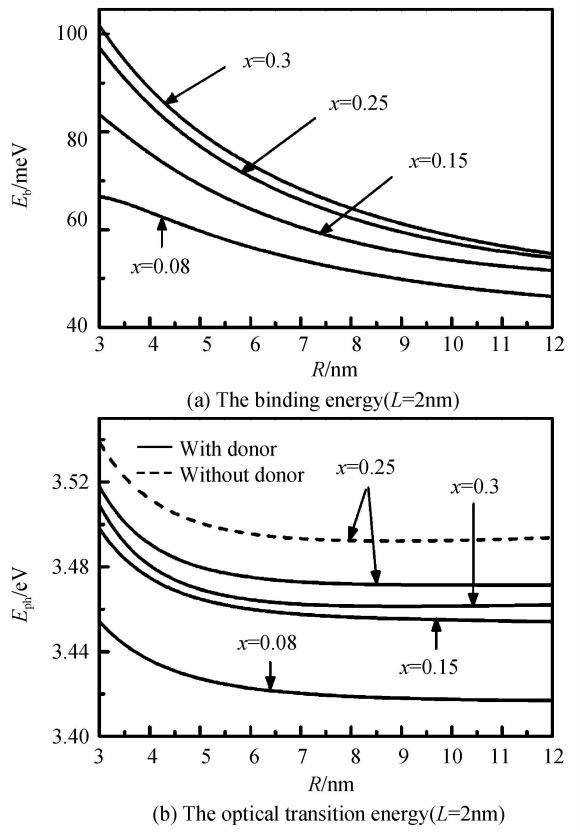

Fig. 3 Variations of the binding energy and optical transition energy as a function of disk radius R when the donor is located at the center of the disk-shaped QDs

In Fig. 3 (b), we can find that the optical transition energy decreases quickly if R (< 5 nm) is increased and decreases slowly if R is further increased (R > 5 nm), and it is insensitive to the disk radius when R > 7 nm. This is due to the total confinement energy of the electron and hole carriers decreases rapidly when R(< 5 nm) is increased and decreases at a slower rate if R is further increased (R > 5 nm) (see Fig. 4). Moreover, we also find from Fig. 3(b) that in the disk-shaped QDs with L = 2 nm, the optical transition energy has a blue-shift for any disk radius when Mg composition increases from 0.08 to 0.25 because of the strong localization of the electron and hole wave functions in the disk-shaped QD. However, the optical transition energy has a red-shift if Mg composition x further increases from 0.25 to 0.3. Also, Fig. 3(b) indicates that the incorporation of the ionized donor in the disk- shaped QDs can obviously reduce the optical transition energy for any disk radius when L = 2 nm, which is consistent with Fig. 2(b).

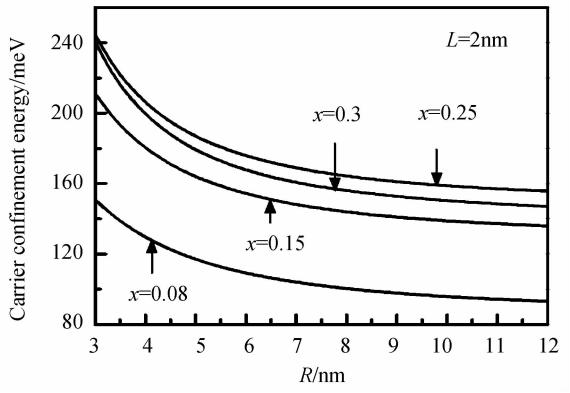

Fig. 4 The carrier confinement energy as a function of disk radius R when the donor is located at the center of the disk-shaped QDs

Fig. 5 presents the variation of the binding energy of (D^+ X) E_b and the optical transition energy E_{ph} as a function of the donor position z_0 in strained WZ ZnO/$Mg_xZn_{1-x}O$ disk-shaped QDs with height L = 2 nm and radius R = 10 nm for three different Mg compositions: 0.15, 0.25 and 0.3. It is observed from Fig. 5 that in all case the binding energy of (D^+ X) (the optical transition energy) firstly increases (decreases) when the ionized donor is moved from the left barrier to the right barrier along the growth axis of the disk-shaped QD, and reaches its maximum (minimum) when the donor located in the vicinity of the left interface of the disk-shaped QDs, and then reduces (increases) to the minimum (maximum) values when the donor located in the vicinity of the right interface of the disk-shaped QDs. and again increase (decrease). The physical reason can be understood as follows. The strong BEF breaks the parity of the disk-shaped QD potential. The electron wave function $h(z_e)$ is localized inside of the disk-shaped QD, close to the left interface. Correspondingly, the hole wave function $h(z_h)$ is located close to the right interface (Fig. 2 of Ref. [22]). The Coulomb interaction between the electron (hole) and the donor is strongly influenced by the position, which, in turn, has a large influence on the interband optical transition. The Coulomb attractive interaction between the electron and the ionized donor enhances if the ionized donor is moved from the left barrier of the disk-shaped QD to right along z-direction (z_0 < (L/2 nm). The electron probability has its maximum approximately at the left interface of disk-shaped QD. As a result, the binding energy increases, and the optical transition energy decreases. As the donor is continuously moved toward right in the disk-shaped QD along z-direction ((L/2 nm < z_0 < L/2

nm), the coulomb attractive (repulsive) interaction between the electron (hole) and the donor decreases (increases). Hence the (D^+ X) complex has higher ground-state energy, which will lead to the decreasing of the binding energy and the increase in the optical transition energy. Correspondingly, when the ionized donor is further moved from the right interface to the right barrier of the disk-shaped QDs ($z_0 > L/2$ nm), the binding energy is dominated by the donor-hole Coulomb repulsive interaction, which causes the optical transition energy reduces. We thus have the important conclusion that the optical properties of (D^+ X) complex sensitively depend on the donor position in the WZ ZnO/$Mg_xZn_{1-x}O$ disk-shaped QDs. Moreover, we also observe from Fig. 5 that the influence of Mg composition on E_b is more remarkable when the donor is localized in the vicinity of the left interface of the disk-shaped QDs, whereas the influence of Mg composition on E_{ph} is more prominent when the donor is localized in the vicinity of the right interface of the disk-shaped QDs.

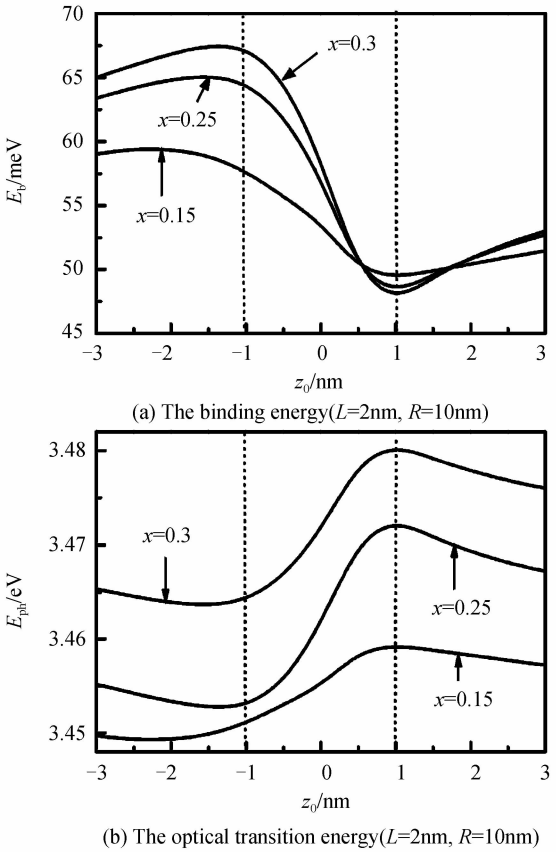

Fig. 5 The binding energy and optical transition energy as a function of the donor position z_0 in the disk-shaped QDs

We plot in Fig. 6 the curves of the oscillator strength versus disk height L and disk radius R when the donor is located at the center of strained WZ ZnO/$Mg_xZn_{1-x}O$ disk-shaped QDs for different Mg compositions. From Fig. 6(a), it is found that the oscillator strength reduces with the increasing disk height L in all case, especially for the disk-shaped QDs with higher Mg composition (x=0.25 and 0.3), and it comes to zero when the disk height approaches to 5.5 nm. The oscillator strength reduces with increasing Mg composition. Fig. 6(b) shows that the oscillator strength is insensitive to the disk radius for all Mg composition. For all we know, the oscillator strength is sensitively dependent on the confinement of the electron and the hole and the overlap between them. Moreover, the BEF affects the confinement of the electron and the hole and the recombination rate of the electron and the hole. These factors lead to the variation of the oscillator strength.

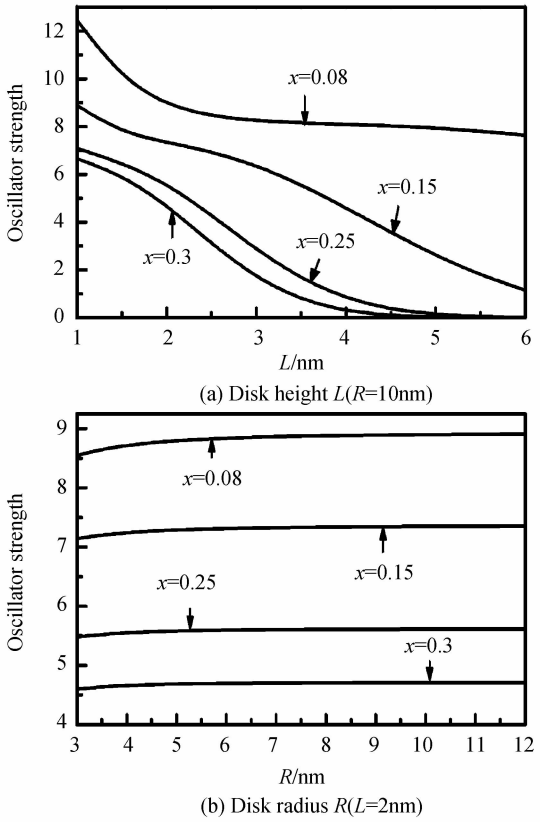

Fig. 6 The oscillator strength as functions of disk height L and disk radius R when the donor is located at the center of the disk-shaped QDs

The calculated radiative lifetime τ of (D^+ X) complex is plotted in Fig. 7 as functions of disk height L and disk radius R when the donor is located at the center of strained WZ ZnO/$Mg_xZn_{1-x}O$ disk-shaped QDs for different Mg compositions x. As an important physical quantity, the radiative lifetime is inversely proportional to the oscillator strength and the square of the optical transition energy (refer to Eq. (11)). We can see from Fig. 7(a) that the radiative lifetime increases with increasing the disk height L. It is worthwhile to note that the radiative lifetime increases

very smoothly with the increasing of the disk height for the disk-shaped QDs with low Mg composition ($x=0.08$), and it increases four orders of magnitude when the disk height L increases from 1 nm to 5 nm for the high Mg composition QDs ($x=0.25$ and 0.3). For instance, for $x=0.08$ case, the net enhancement of $\Delta\tau$ is of 83 ps with percentage of 63.8% for the two cases of $L=1$ nm and 5 nm. The corresponding difference is of 80.7 ns (3.8×10^4%) for the $x=0.3$ case. The reason is attributed to the reductions of the oscillator strength of (D^+X) complex and the optical transition energy due to a strong BEF induced by the PE and SP polarizations. Fig. 7(a) also demonstrates that the radiative lifetime increases with increasing Mg composition for a given L, and the increment tendency is more prominent for larger disk height. For example, when Mg composition increases from $x=0.08$ to 0.3, at $L=2$ nm, the deference of the radiative lifetime is $\Delta\tau=156$ ps, whereas the corresponding difference $\Delta\tau=80.7$ ns increases 517.3 times when L increases from $L=2$ to 5 nm. The reason is associated with the competition effects between the quantum confinement and the strong BEF. Moreover, we can see from Fig. 7(b) that the radiative lifetime is insensitive to the disk radius for all case . This is mainly because the optical transition energy and the oscillator strength are both insensitive to the disk radius (see Fig. 3(b) and Fig. 6(b)). Fig. 7(b) also indicates that the radiative lifetime increases with increasing Mg composition for any disk radius when $L=2$ nm. We have thus conclusion that the disk height and Mg composition have significant effects on the optical properties of (D^+X) complex in strained WZ ZnO/$Mg_xZn_{1-x}O$ disk-shaped QD.

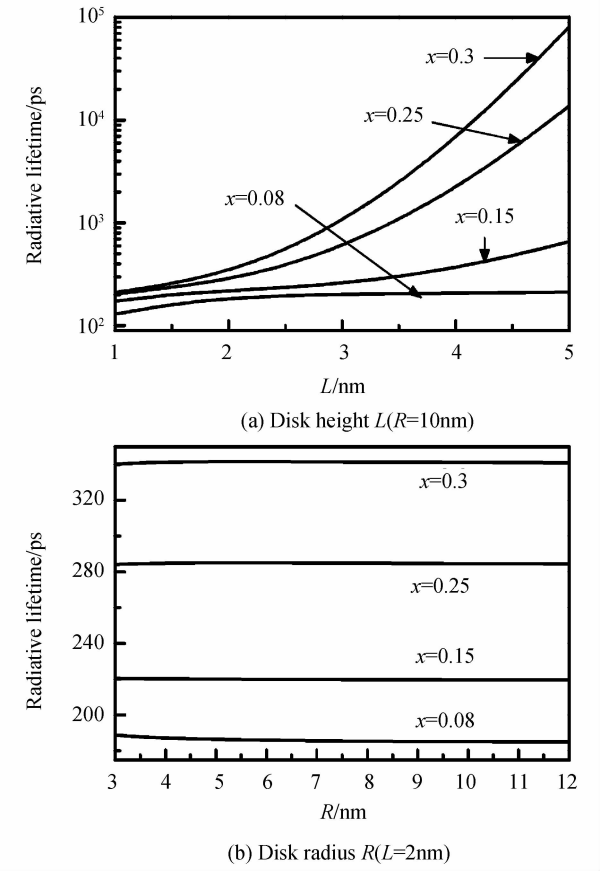

Fig. 7 Variations of the radiative lifetime as functions of disk height L and disk radius R when the donor is located at the center of the disk-shaped QDs

3 Conclusions

Within the framework of the effective-mass approximation, we have presented a calculation of the binding energy, the optical transition energy, the oscillator strength and the radiative lifetime of ionized donor bound exciton (D^+X) in a strained WZ ZnO/$Mg_xZn_{1-x}O$ quantum dot (QD), assumed to be in the form of a disk, with finite potential barriers at all surface, for the case of a ionized donor located on the axis of the disk. The calculations have been performed by using a suitable variational wave function, which take into account the confinement of the carriers in the disk (axial and radial), and the influence of the Coulomb interactions between the donor and the electron (hole) and between the electron and the hole. Moreover, the strong BEF induced by the SP and PE polarizations is considered. The results show that the disk structural parameters (height L and Mg composition x in the barrier) and the donor position have a strong influence on the binding energy E_b, optical transition energy E_{ph}, oscillator strength $f_{(D^+X)}$, and radiative lifetime τ of (D^+X) complex. As the disk height increases, the binding energy, optical transition energy, and oscillator strength both decrease, whereas the radiative lifetime increases. The influences of disk height on E_b, E_{ph}, $f_{(D^+X)}$, and τ become more prominent for the disk-shaped QDs with higher Mg composition. The binding energy of (D^+X) complex decreases with increasing disk radius, whereas the optical transition energy, oscillator strength, and radiative lifetime are both insensitive to the disk radius for different Mg compositions. E_b(E_{ph}) has a maximum (minimum) when the donor is located in the vicinity of the left interface of the disk-shaped QDs. On the contrary, E_b(E_{ph}) has a minimum (maximum) when the donor is located in the vicinity of the right interface of the disk-shaped QDs. Therefore, in order to obtain a short-wavelength optical device, we should choose the suitable disk height, Mg composition in the barrier and the ionized donor position. It is hoped that the results on the optical properties of ionized donor bound exciton in Mg based ZnO semiconducting material will kindle more outcomes in experimental aspects in future.

References

[1] WEI Z P, YAO B, ZHANG Z Z, *et al*. Formation of *p*-type MgZnO by nitrogen doping[J]. *Applied Physics Letters*, 2006, **89**(10): 102104.

[2] BELGHAZI Y, SCHMERBER G, COLIS S, *et al*. Extrinsic origin of ferromagnetism in ZnO and $Zn_{0.9}Co_{0.1}O$ magnetic semiconductor films prepared by sol-gel technique[J]. *Applied Physics Letters*, 2006, **89**(12): 122504.

[3] BHOSLE V, TIWARI A, NARAYAN J. Electrical properties of transparent and conducting Ga doped ZnO[J]. *Journal of Applied Physics*, 2006, **100**(3): 033713.

[4] WANG Ma-hua, ZHU Guang-ping, XU Chun-xiang. Photoluminescent properties in Manganese-doped Zinc Oxide tetropods[J]. *Acta Photonica Sinica*, 2010, **39**(1): 25-29.

[5] GOLD A. Transport properties of the electron gas in ZnO/MgZnO heterostructures[J]. *Applied Physics Letters*, 2010, **96**(24): 242111.

[6] LANGE M, KUPPER J, DIETRICH C P, *et al*. Exciton localization and phonon sidebands in polar ZnO/MgZnO quantum wells[J]. *Physical Review B*, 2012, **86**(4): 045318.

[7] STÖLZEL M, MÜLLER A, BENNDORF G, *et al*. Determination of unscreened exciton states in polar ZnO/(Mg, Zn)O quantum wells with strong quantum-confined Stark effect[J]. *Physical Review B*, 2013, **88**(4): 045315.

[8] PULS J, SADOFEV S, SCHÄFER P, *et al*. Optical in-plane anisotropy of ZnO/(Zn, Mg)O quantum wells grown on *a*-plane sapphire: Implications for optical spin control[J]. *Physical Review B*, 2014, **89**(8): R081301.

[9] BÉAUR L, BRETAGNON T, GIL B, *et al*. Exciton radiative properties in nonpolar homoepitaxial ZnO/(Zn,Mg)O quantum wells[J]. *Physical Review B*, 2011, **84**(16): 165312.

[10] PARK S H. Electronic and optical properties of ZnO/ZnMgO quantum well lasers with piezoelectric and spontaneous polarizations[J]. *Journal of the Korean Physical Society*, 2007, **50**(1): 16-20.

[11] XU T N, WU H Z, QIU D J, *et al*. Calculation of excitonic transitions in ZnO/MgZnO quantum-well heterostructures [J]. *Chinese Physics Letters*, 2003, **20**(10): 1829-1832.

[12] STÖLZEL M, KUPPER J, BRANDT M, *et al*. Electronic and optical properties of ZnO/(Mg,Zn)O quantum wells with and without a distinct quantum-confined Stark effect[J]. *Journal of Applied Physics*, 2012, **111**(6): 063701.

[13] MORHAIN C, BRETAGNON T, LEFEBVRE P, *et al*. Internal electric field in wurtzite $ZnO/Zn_{0.78}Mg_{0.22}O$ quantum wells[J]. *Physical Review B*, 2005, **72**(24): R241305.

[14] MAKINO T, TUAN N T, SUN H D, *et al*. Temperature dependence of near ultraviolet photoluminescence in ZnO/(Mg,? Zn)O multiple quantum wells[J]. *Applied Physics Letters*, 2001, **78**(14): 1979-1981.

[15] PARK S H, AHN D. Spontaneous and piezoelectric polarization effects in wurtzite ZnO/MgZnO quantum well lasers[J]. *Applied Physics Letters*, 2005, **87**(25): 253509 (1-3).

[16] BRETAGNON T, LEFEBVRE P, VALVIN T, *et al*. Time resolved photoluminescence study of ZnO/(Zn, Mg)O quantum wells[J]. *Journal of Crystal Growth*, 2006, **287**: 12-15.

[17] DIJKEN A, MEULENKAMP E A, VANMAEKELBERGH D, *et al*. The kinetics of the radiative and nonradiative processes in nanocrystalline ZnO particles upon photoexcitation[J]. *Journal of Physical Chemistry B*, 2000, **104**: 1715-1723.

[18] QIAO Q, LI B H, SHAN C X, *et al*. Light-emitting diodes fabricated from small-size ZnO quantum dots[J]. *Materials Letters*, 2012, **74**: 104-106.

[19] WEI S Y, WEI L L, XIA C X, *et al*. Exciton states and interband optical transitions in ZnO/MgZnO quantum dots [J]. *Journal of Luminescence*, 2008, **128**: 1285-1290.

[20] ZHAO X, WEI S Y, XIA C X, *et al*. Optical properties of excitoncon finement in wurtzite $ZnO/Mg_xZn_{1-x}O$ coupled quantum dots [J]. *Journal of Luminescence*, 2011, **131**: 297-300.

[21] ZHAO X, WEI S Y, XIA C X. Influence of Mg content on optical properties of exciton confinement in wurtzite $ZnO/Mg_xZn_{1-x}O$ coupled quantum dots[J]. *Superlattices and Microstructures*, 2011, **50**: 207-214.

[22] ZHENG D M, WANG Z C. Influence of Mg composition on optical properties of exciton confinement in strained wurtzite $ZnO/Mg_xZn_{1-x}O$ cylindrical quantum dots[J]. *Communications in Theoretical Physics*, 2012, **58**(6): 915-922.

[23] MINIMALA N S, JOHN PETE A, LEE C W. Electric field induced nonlinear optical properties of a confined exciton in a $ZnO/Mg_xZn_{1-x}O$ strained quantum dot[J]. *Physica E*, 2013, **48**: 133-139.

[24] LEE J K, NASTASI M, HAMBY D W, *et al*. Optical observation of donor-bound excitons in hydrogen-implanted ZnO[J]. *Applied Physics Letters*, 2005, **86**(17): 171102.

[25] MEYER B, SANN J, LAUTENSCHLÄGER S, *et al*. Ionized and neutral donor-bound excitons in ZnO[J]. *Physical Review B*, 2007, **76**(18): 184120.

[26] MEYER B K, SANN J, EISERMANN S, *et al*. Excited state properties of donor bound excitons in ZnO[J]. *Physical Review B*, 2010, **82**(11): 115207.

[27] CHEN S L, CHEN W M, BUYANOVA I A. Donor bound excitons involving a hole from the B valence band in ZnO: Time resolved and magneto-photoluminescence studies[J]. *Applied Physics Letters*, 2011, **99**(9): 091909.

[28] CHEN S L, CHEN W M, BUYANOVA I A. Dynamics of donor bound excitons in ZnO[J]. *Applied Physics Letters*, 2013, **102**(12): 121103.

[29] MOHAMMADBEIGI F, SENTHIL KUMAR E, ALAGHA S, *et al*. Carbon related donor bound exciton transitions in ZnO nanowires[J]. *Journal of Applied Physics*, 2014, **116**(5): 053516.

[30] XIU F X, YANG Z, MANDALAPU L J, *et al*. Donor and acceptor competitions in phosphorus-doped ZnO[J]. *Applied Physics Letters*, 2006, **88**(15): 152116.

[31] THOMAS M A, CUI J B. Investigations of acceptor related photoluminescence from electrodeposited Ag-doped ZnO[J]. *Journal of Applied Physics*, 2009, **105**(9): 093533.

[32] YE Z Z, ZENG Y J, LU Y F, *et al*. Donor/acceptor doping and electrical tailoring in ZnO quantum dots[J]. *Applied Physics Letters*, 2007, **91**(11): 112110.

[33] LIU Y M, XIA, C X, WEI S Y. The donor bound exciton states in wurtzite GaN quantum dot[J]. *Current Applied Physics*, 2009, **9**: 39-43.

[34] ZHENG D M, WANG Z C, XIAO B Q. Effects of hydrostatic pressure on ionized donor bound exciton states in strained wurtzite $GaN/Al_xGa_{1-x}N$ cylindrical quantum dots [J]. *Physica B*, 2012, **407**: 4160-4167.

[35] FONOBEROV V A, BALANDIN A A. Origin of ultraviolet photoluminescence in ZnO quantum dots: Confined excitons versus surface-bound impurity exciton complexes[J]. *Applied Physics Letters*, 2004, **85**(24): 5971-5973.

[36] FONOBEROV V A, BALANDIN A A. Excitonic properties of strained wurtzite and zinc-blende $GaN/Al_xGa_{1-x}N$ quantum dots[J]. *Journal of Applied Physics*, 2003, **94**(11): 7178-7186.